Electronic Supplementary Material (ESI) for Journal of Materials Chemistry A.

Supporting Information

Free-standing NiV_2S_4 nanosheet arrays on 3D Ni framework via anion exchange reaction as a novel electrode for asymmetric supercapacitor applications

Rudra Kumar, Prabhakar Rai*, Ashutosh Sharma*

Department of Chemical Engineering, Indian Institute of Technology Kanpur, Kanpur 208016, India

*E-mail: prkrai@iitk.ac.in, ashutos@iitk.ac.in

Figure S1. SEM, elemental mapping, and EDX spectrum of $Ni_3(VO_4)_2$ nanosheet arrays.

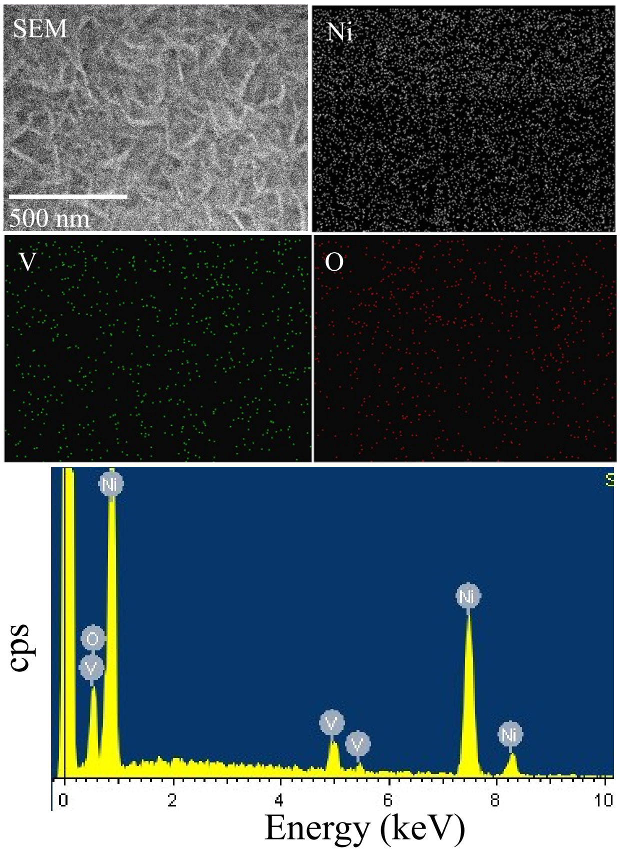

Figure S2. SEM, elemental mapping, and EDX spectrum of NiV_2S_4 nanosheet arrays.

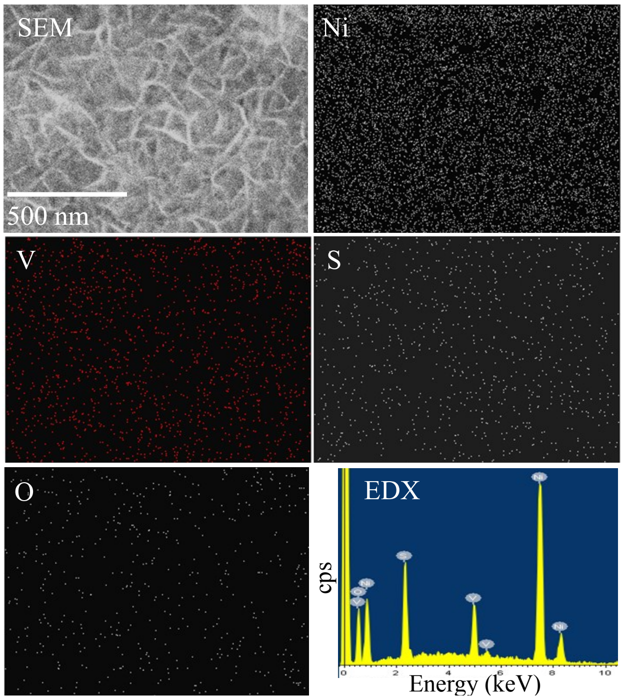

Figure S3. XRD profile of as synthesized NiV_2S_4 nanosheet arrays along with curve from standard PDF card.

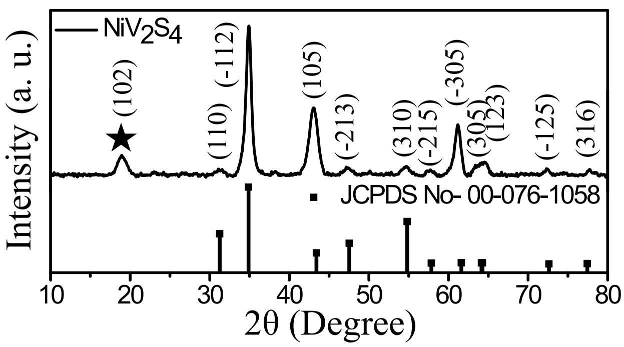

Figure S4. XPS spectra of $Ni_3(VO_4)_2$ nanosheet arrays; a) survay, b) Ni, c) V and d) O.

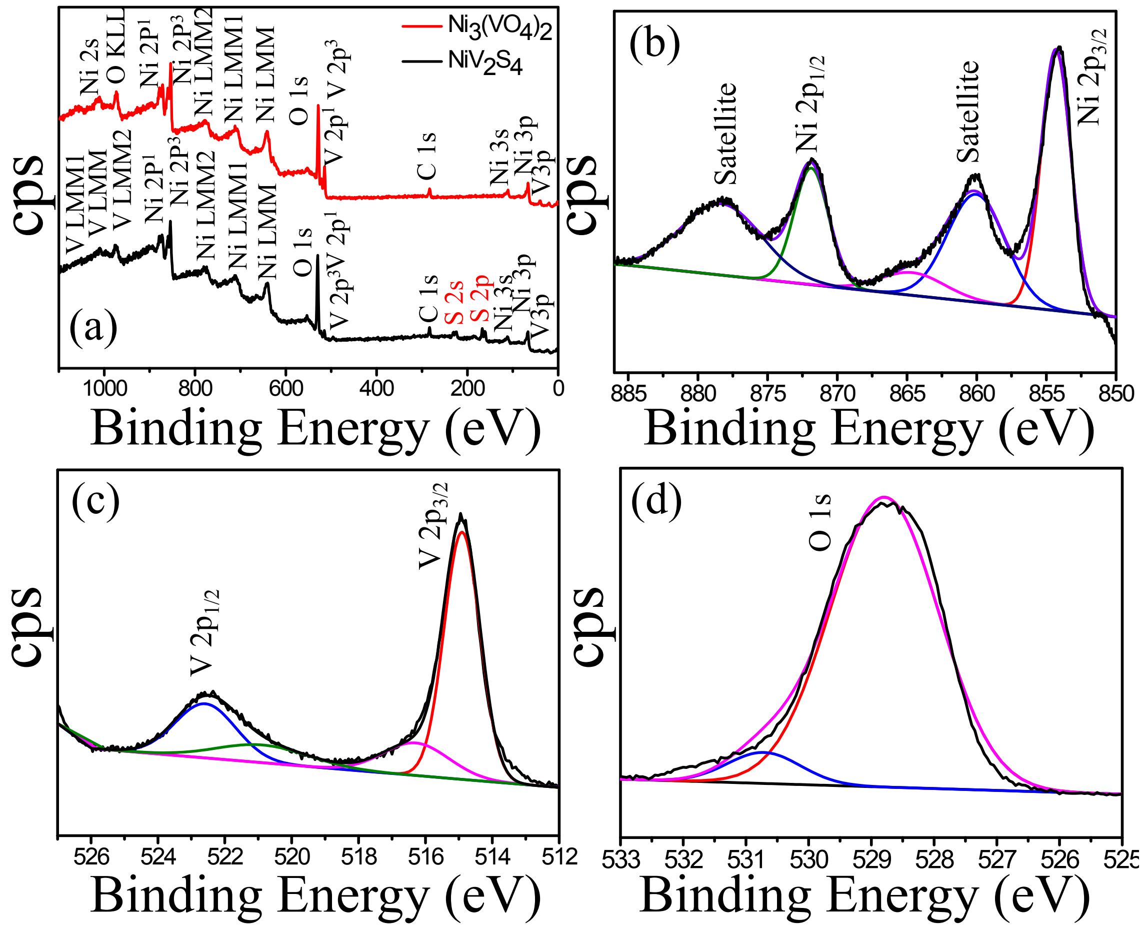

Figure S5. BET surface area and pore size distribution of (a) $Ni_3(VO_4)_2$ and (b) NiV_2S_4 nanosheet arrays.

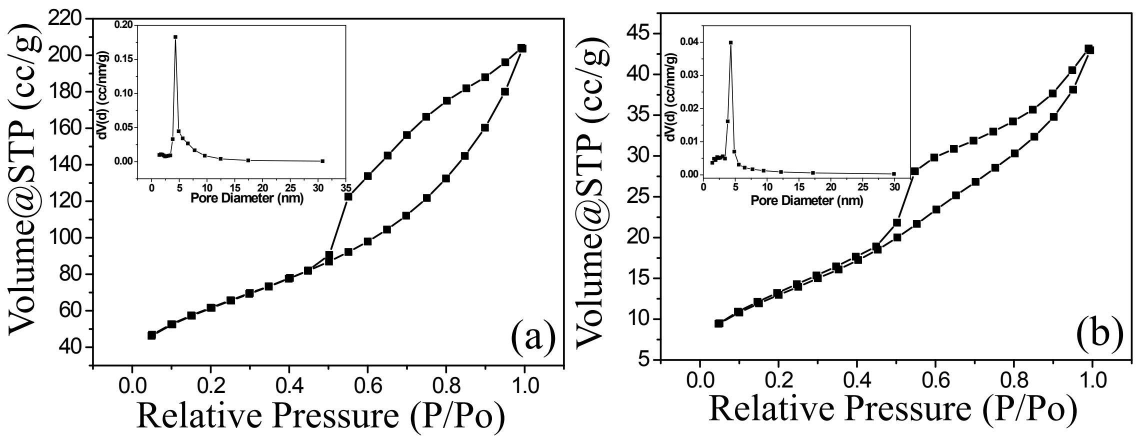

Figure S6. (a) CV and (b) GCD curve of $Ni_3(VO_4)_2$ nanosheet arrays.

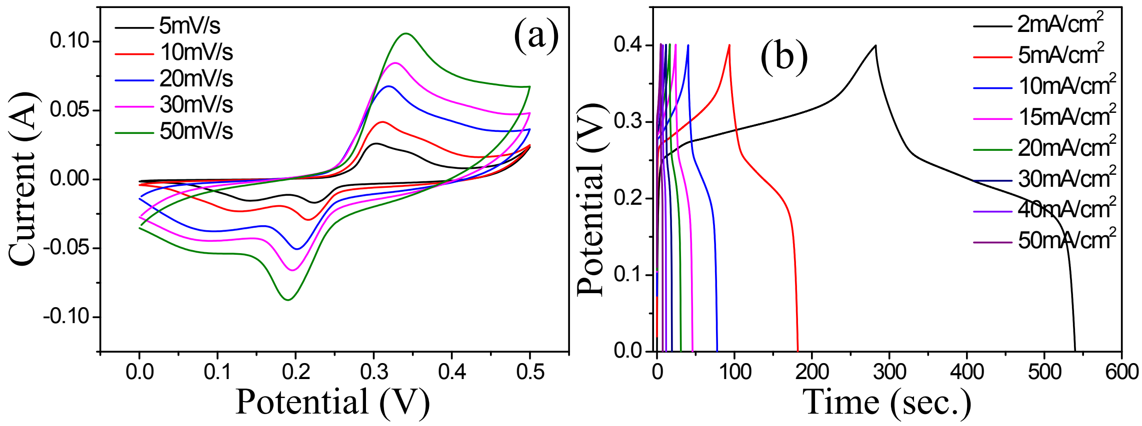

Figure S7. GCD curve of $Ni_3(VO_4)_2$ nanosheet arrays synthesized at different times.

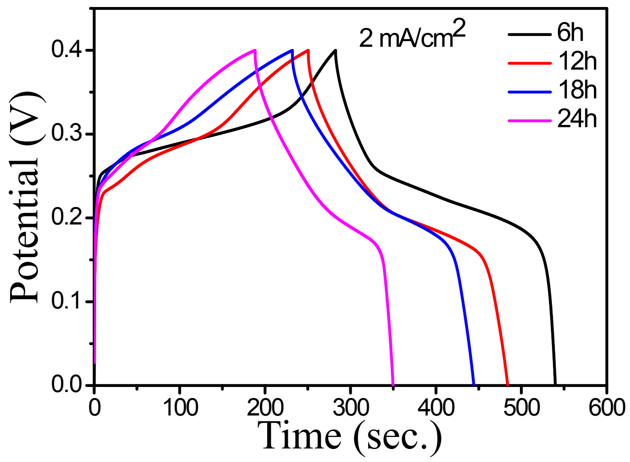

Figure S8. (a) Nyquist plot (inset shows high frequency region) and (b) I-V curve measurement of NiV_2S_4 and $Ni_3(VO_4)_2$ nanosheet arrays.

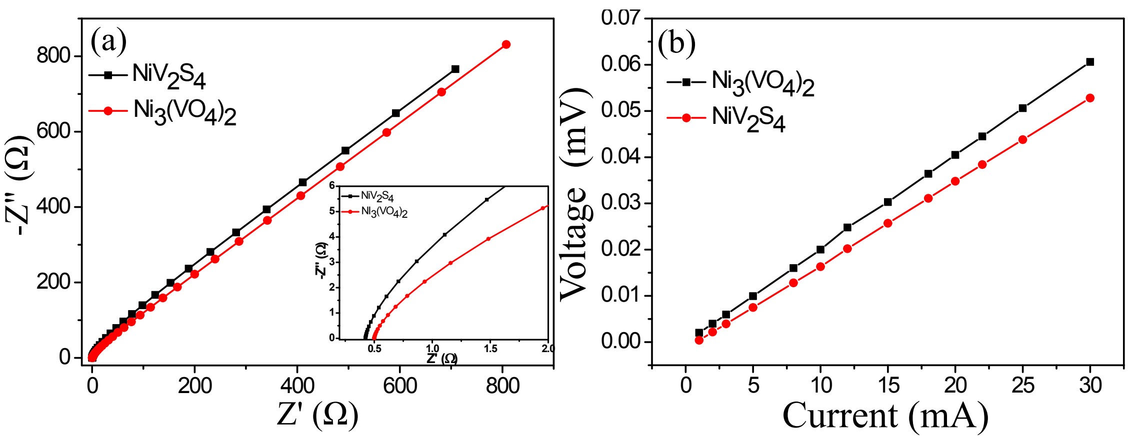

Figure S9. Long term cycling stability of NiV_2S_4 nanosheet array at 50 mVs^{-1}.

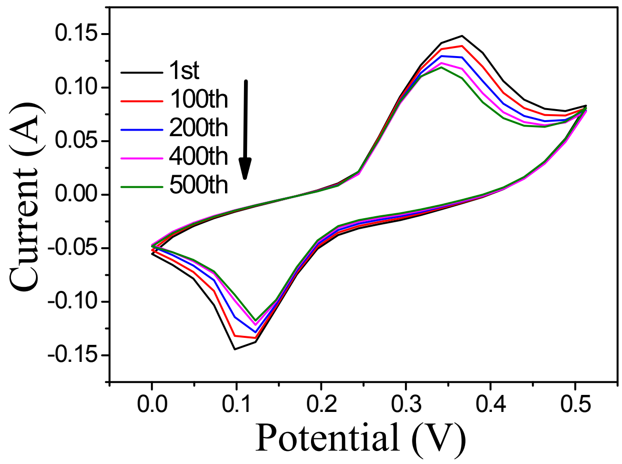

Figure S10. Rate capability of NiV_2S_4 nanosheet array.

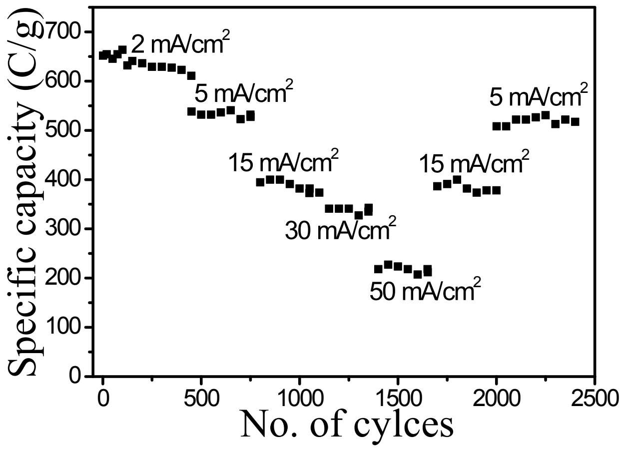

Figure S11. Cycling performance of $Ni_3(VO_4)_2$ nanosheet array at (a) 10 $mAcm^{-2}$ current density for 2000 cycles and (b) 5 $mA.cm^{-2}$ for 500 cycles .

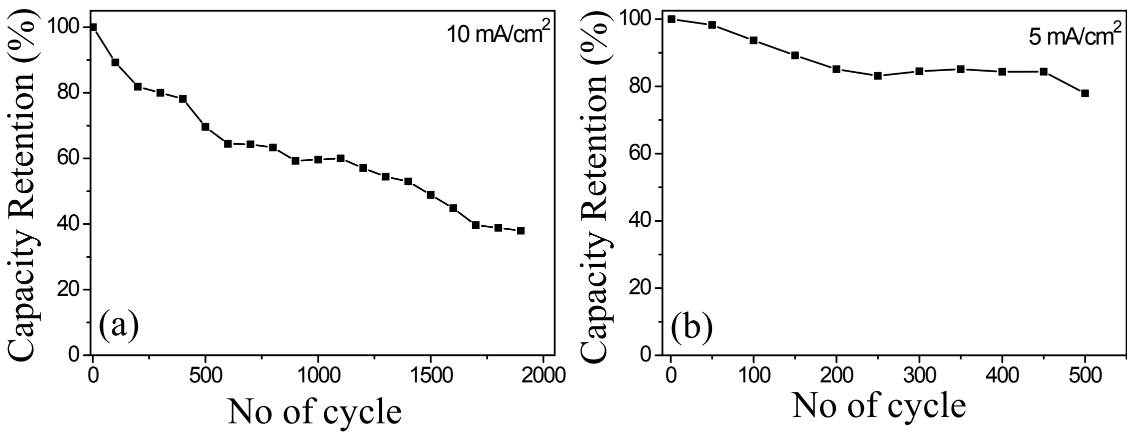

Figure S12. SEM images of (a) $Ni_3(VO_4)_2$, (b) NiV_2S_4, and (c) EIS of NiV_2S_4 after cycling performance at 10 $mAcm^{-2}$ and 30 $mAcm^{-2}$ current density, respectively for 2000 cycles.

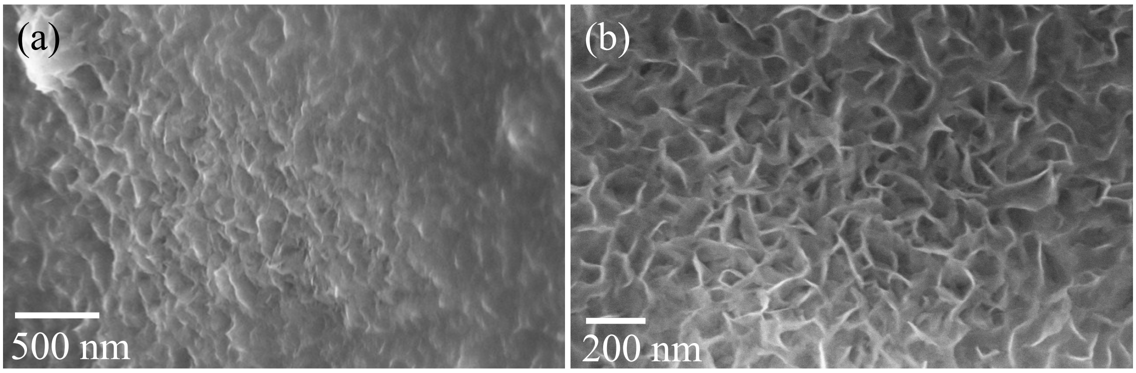

Figure S13. EIS of NiV_2S_4 after cycling performance at 30 $mAcm^{-2}$ current density for 2000 cycles.

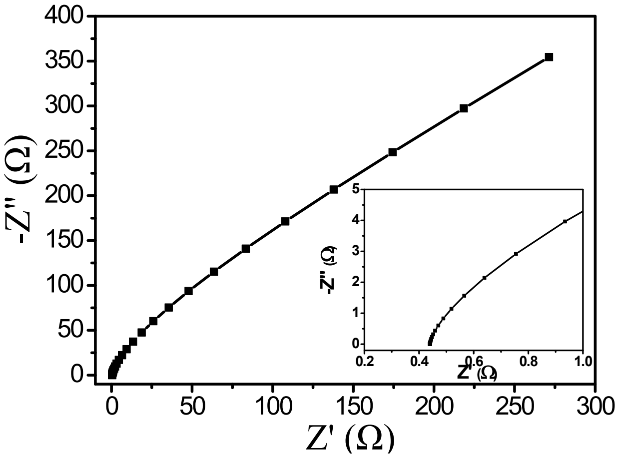

Figure S14. (a) CV curves at different scan rates (5-50 mVs^{-1}), (b) GCD curves at different current densities (1-5 Ag^{-1}) and c) Variation of specific capacity with respect to different current densities for AC.

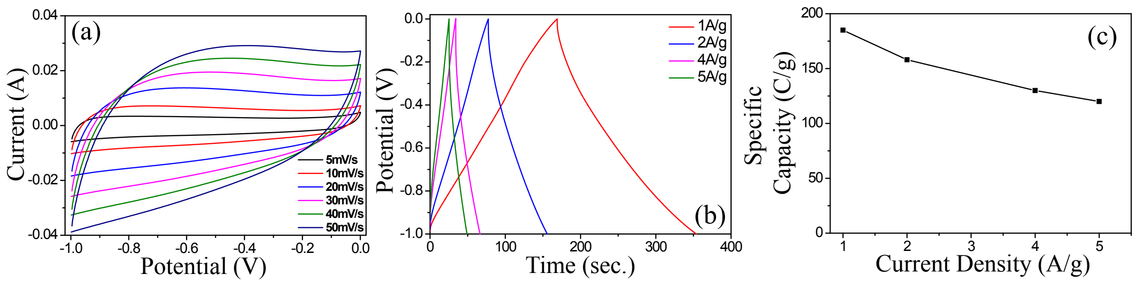

Figure S15: CV of NiV_2S_4 //AC asymmetric supercapacitor at 10 mVs^{-1} at different potential window (1- 1.6 V).

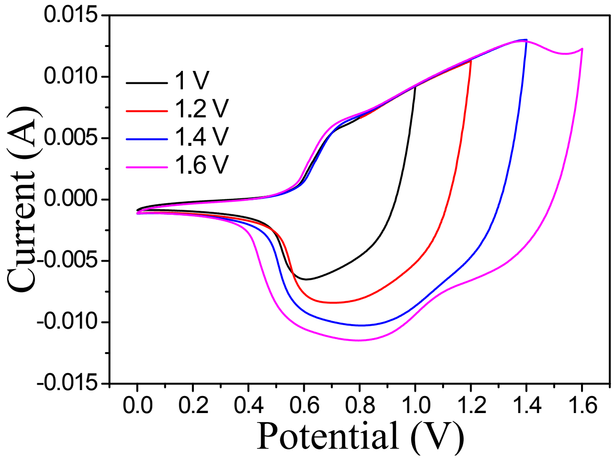

Table S1. Comperative study of different asymmetric supercapacitor performance reported in literature with respect to our electrode.

Asymmetric Supercapacitor	**Voltage (V)**	**Energy Density ($Whkg^{-1}$)**	**Power Density (Wkg^{-1})**	**Cyclic Stability**	**Ref No**
Ni-Co-S nanosheet arrays//graphene	1.8	60	1800	90.1% (10,000)	1
$NiCo_2S_4$ nanotube arrays/Ni foam//RGO	1.6	16.6	2350	92% (5000)	2
$Ni_3(VO_4)_2$//AC	1.6	25.3	240	92% (1000)	3
3D Ni_3S_2 nanosheet arrays on Ni foam//AC	1.6	34.6	150.4	85.7 % (1000)	4
$NiCo_2S_4$@$Ni_3V_2O_8$ on Ni foam//AC	1.6	42.7	200	90% (5000)	5
$NiCo_2S_4$//AC	1.5	28.3	245	91.7% (5000)	6

$Ni(OH)_2$/graphene//graphene	1.6	77.8	175	94%(3000)	7
Co_9S_8 nanoflakes//AC	1.6	31.4	200	90% (5000)	8
Core-shell $NiCo_2S_4$//C	1.6	22.8	160		9
Hollow hetero Ni_7S_6/Co_3S_4 nanoboxes//AC	1.5	31	180	86% (5000)	10
rGO-Ni_3S_2//AC	1.6	37.19	399.9	85.6% (5000)	11
Ni@rGO−Co_3S_4// Ni@rGO−Ni_3S_2	1.3	55.16	965	96.2 % (3000)	12
Capsule-like porous hollow $Ni_{1.77}Co_{1.23}S_4$ // AC	1.6	42.7	190.8		13
Ni–Co sulphide nanowires//AC	1.8	25	447	73.1% (3000)	14
NiV_2S_4//AC	1.6	45.2	240	90.7% (1000)	This Work

References

1. W. Chen, C. Xia and H. N. Alshareef, *ACS Nano*, 2014, **8**, 9531-9541.
2. H. Chen, J. Jiang, L. Zhang, D. Xia, Y. Zhao, D. Guo, T. Qi and H. Wan, *J. Power Sources*, 2014, **254**, 249-257.
3. R. Kumar, P. Rai and A. Sharma, *J. Mater. Chem. A*, 2016, **4**, 9822-9831.
4. H. Huo, Y. Zhao and C. Xu, *J. Mater. Chem. A*, 2014, **2**, 15111-15117.
5. L. Niu, Y. Wang, F. Ruan, C. Shen, S. Shan, M. Xu, Z. Sun, C. Li, X. Liu and Y. Gong, *J. Mater. Chem. A*, 2016, **4**, 5669-5677.
6. Y. Zhu, Z. Wu, M. Jing, X. Yang, W. Song and X. Ji, *J. Power Sources*, 2015, **273**, 584-590.
7. J. Yan, Q. Wang, T. Wei and Z. C. Fan, *Adv. Energy Mater.*, 2014, **4**, 1300816.
8. R. B. Rakhi, N. A. Alhebshi, D. H. Anjum and H. N. Alshareef, *J. Mater. Chem. A*, 2014, **2**, 16190-16198.

9. W. Kong, C. Lu, W. Zhang, J. Pu and Z. Wang, *J. Mater. Chem. A*, 2015, **3**, 12452-12460.
10. H. Hua, S. Liu, Z. Chen, R. Bao, Y. Shi, L. Hou, G. Pang, K. N. Hui, X. Zhang and C. Yuan, *Sci. Rep.*, 2016, **6**, 20973.
11. H. Lin, F. Liu, X. Wang, Y. Ai, Z. Yao, L. Chu, S. Han and X. Zhuang, *Electrochim. Acta*, 2016, **191**, 705-715.
12. D. Ghosh and C. K. Das, *ACS Appl. Mater. Interface*, 2015, **7**, 1122-1131.
13. Y. Tang, S. Chen, S. Mu, T. Chen, Y. Qiao, S. Yu and F. Gao, *ACS Appl. Mater. Interface*, 2016, **8**, 9721-9732.
14. Y. Li, L. Cao, L. Qiao, M. Zhou, Y. Yang, P. Xiao and Y. Zhang, *J. Mater. Chem. A*, 2014, **2**, 6540-6548.